

PAPER • OPEN ACCESS

## Direct polymer microcantilever fabrication from free-standing dry film photoresists



To cite this article: Madeleine Nilsen *et al* 2020 *J. Micromech. Microeng.* **30** 095012

View the [article online](#) for updates and enhancements.

### You may also like

- [Strongly anisotropic thermal conductivity and adequate breathability of bilayered films for heat management of on-skin electronics](#)  
Tianle Zhou, Hao Wei, Huaping Tan et al.
- [Microfabrication of bulk PZT transducers by dry film photolithography and micro powder blasting](#)  
I Misri, P Hareesh, S Yang et al.
- [Print-to-pattern dry film photoresist lithography](#)  
Shaun P Garland, Terrence M Murphy and Tingrui Pan

# Direct polymer microcantilever fabrication from free-standing dry film photoresists

Madeleine Nilsen<sup>1</sup> , Oliver Dannberg<sup>2</sup>, Thomas Fröhlich<sup>2</sup> and Steffen Strehle<sup>3</sup> 

<sup>1</sup> Ulm University, Institute of Electron Devices and Circuits, Albert-Einstein-Allee 45, 89081 Ulm, Germany

<sup>2</sup> Technische Universität Ilmenau, Institute for Process Measurement and Sensor Technology, Ilmenau 98693, Germany

<sup>3</sup> Technische Universität Ilmenau, Institute of Micro-and Nanotechnologies MacroNano<sup>®</sup>, Ilmenau 98693, Germany

E-mail: [steffen.strehle@tu-ilmenau.de](mailto:steffen.strehle@tu-ilmenau.de)

Received 13 March 2020, revised 15 May 2020

Accepted for publication 18 June 2020

Published 30 June 2020



CrossMark

## Abstract

Traditionally, polymeric microcantilevers are assembled by a multitude of process steps comprising liquid spin-coated photoresists and rigid substrate materials. Polymer microcantilevers presented in this work rely instead on commercially available dry film photoresists and allowed an omission of multiple fabrication steps. Thin, 5  $\mu\text{m}$  thick dry film photoresists are thermally laminated onto prepatterned silicon substrates that contain AFM compatible probe bodies. Partially suspended dry film resists are formed between these probe bodies, which are patterned to yield microcantilevers using conventional photolithography protocols. A limited amount of thermal cycling is required, and sacrificial probe-release layers are omitted as microcantilevers form directly through resist development. Even 1 mm long polymeric cantilevers were fabricated this way with superior in-plane alignment. The general effects of post-exposure bake (PEB) and hardbake protocols on cantilever deflection are discussed. Generally, higher PEB temperatures limit out-of-plane cantilever bending. Hardbake improved vertical alignment only of high-PEB temperature cantilevers, while surprisingly worsening the alignment of low-PEB temperature cantilevers. The mechanism behind the latter is likely explained by complex interactions between the resist and the substrate related to differences in thermal expansion, heat conduction, as well as resist cross-linking gradients. We present furthermore multilayer structures of dry film resists, specifically cylindrical dry film resist pillars on the polymer cantilever, as well as the integration of metal structures onto the polymer cantilever, which should enable in future integrated piezoresistive deflection readout for various sensing applications. Finally, cantilever spring constants were determined by measuring force–displacement curves with an advanced cantilever calibration device, allowing also the determination of both, dry film resist cantilever density and Young's modulus.

Supplementary material for this article is available [online](#)

Keywords: polymer cantilever, dry film photoresist, photolithography, AFM, piezoresistive

(Some figures may appear in colour only in the online journal)



Original content from this work may be used under the terms of the [Creative Commons Attribution 4.0 licence](#). Any further distribution of this work must maintain attribution to the author(s) and the title of the work, journal citation and DOI.

## 1. Introduction

The invention of atomic force microscopy (AFM) in 1986 greatly contributed to surface science and fostered micro-fabrication technology and the commercial availability of microcantilever beams. AFM cantilevers of either silicon or silicon nitride are by far the most popular and rely on a processing fully compatible with modern integrated circuit fabrication technology. However, both materials have a relatively high Young's modulus, expected in the range of 150 to 300 GPa [1]. Such relatively stiff beams are generally useful for many AFM applications, but appear less advantageous in applications monitoring minute forces or changes of the cantilever beam deflection. A notable example is here the detection of various chemical and biochemical species. Target molecules preferentially attach to one side of the cantilever beam, and create a differential surface stress  $\Delta\sigma$  over the opposite cantilever faces, with a resulting vertical beam deflection  $\Delta z$  according to equation (1) [2]:

$$\Delta z = \frac{3(1-\nu)L^2}{Et^2} \Delta\sigma \quad (1)$$

where  $E$ ,  $\nu$ ,  $t$  and  $L$  are the cantilever's Young's modulus, Poisson ratio, beam thickness and length, respectively. In order to enhance the overall deflection sensitivity, researchers have turned to microcantilevers made from various polymers with relatively low stiffness [3]. By far, the most popular choice of a polymer is given by SU-8 photoresist, which is relatively biocompatible [4], supports a lowering of fabrication costs compared to the conventional silicon-based materials [3, 5], is compatible with conventional photolithography, and importantly, exhibits a low Young's modulus if compared to silicon-based materials, of typically less than 5 GPa. Polymer microcantilevers with a piezoresistive element are also interesting as they support sensor compactness, relying on integrated and electronic monitoring of the beam deflection instead of the typical optical detection principle frequently associated with AFM, involving a bulky laser and photodiode system. A recent review paper on SU-8 cantilevers with piezoresistive read-out emphasizes the current attention to the topic [3]. Piezoresistive polymer cantilevers have for example been used to detect traces of explosives [6], CO gas [7] and humidity [8] to mention a few. Besides piezoresistive readout, other compact systems for monitoring cantilever deflection were shown also in combination with polymeric microcantilevers comprising common optical readout strategies and even integrated waveguides [9].

A typical process flow to create tipless SU-8 cantilevers begins by spin-coating the liquid resist onto a planar silicon bulk substrate, followed by mask-assisted UV-exposure and a post-exposure bake (PEB). Also scanning tips, as required for AFM, can be made in principle from the same SU-8 [10], but such cantilevers are not considered in the following. The probe body is created by spin-coating and patterning of a second SU-8 layer on-top of the cantilever structure. Both SU-8 layers are developed either simultaneously [11, 12] or separately [13] to form the complete polymer cantilever probes. Adequate pretreatment of the substrate surface is crucial to

ensure successful release of the developed microcantilever probes. Generally, two main approaches were demonstrated previously, relying on either a dry or wet release approach. In dry release, the substrate is coated with a low free-energy film, such as fluorocarbons, facilitating a mechanical removal of the microcantilever probes by means of tweezers or a razor blade [13, 14]. Wet release requires a sacrificial layer deposited on the substrate, such as a metal [11, 15], silicon oxide [16, 17], polysilicon [18], another polymer like PMMA [13], or Omni-Coat (by Kayaku Advanced Materials) [13, 19]. Removal of this sacrificial layer yields automatically the release of the cantilever probes from the substrate surface. Realizing any of the aforementioned release approaches is possible within most well-equipped cleanrooms, yet both methods of wet and dry release have certain inherent disadvantages. A complete avoidance of plastic deformation of the microcantilevers within a dry release scheme is challenging [5, 13]. For the wet release strategy there are reports on cantilevers sticking to the probe bodies [20] and partly low device yields [17], even though high yields were realized recently with a PMMA sacrificial layer [13]. Both methods suffer furthermore from residual stresses in the released probes. This is mainly caused by a mismatch in coefficients of thermal expansion (CTE) between the utilized photoresist and the bulk substrate during thermal cycling (e.g. for photoresist preparation or hard bake), as well as by gradients in the solvent content in the photoresist leading to non-uniform shrinkage and differences in thermal properties across the cross-section of the cantilevers [5]. The effect of PEB and hardbake on cantilever out-of-plane alignment, as well as storage conditions and time stability have already been thoroughly investigated by several research groups [5, 13, 17]. Their studies demonstrate the fabrication of straight and mechanically similar batches of polymer microcantilevers by a spin-coating strategy, but discuss as well the inherent difficulties and challenges.

To decrease the amount and impact of thermal cycling, to avoid a direct attachment of photoresist to substrate, as well as to eliminate the need for a substrate release layer, we devised a strategy based on dry film photoresist lithography. Within this protocol, a solid sheet of commercially available, 5  $\mu\text{m}$  thick dry film photoresist with excellent thickness uniformity and 2  $\mu\text{m}$  achievable patterning resolution ability is thermally laminated onto a silicon bulk substrate containing pre-patterned AFM compatible probe bodies. Suspended dry resist membranes are created in this manner between those probe bodies, which do not directly adhere to the silicon substrate. Conventional UV-photolithography forms freestanding polymer cantilevers conveniently by UV-exposure, PEB and development directly of these suspended dry resist membranes. The resulting dry resist microcantilevers are already attached to silicon probe bodies, requiring no additional release strategy. The rest of our dry resist protocol shares resemblance to the spin-coating strategy, exchanging only spin-coating and soft-bake by a simple thermal lamination process. No additional equipment is required for dry film photoresist lithography besides an inexpensive thermal roller laminator, supporting facile integration of dry film photoresist technology to the lithography lab.

Polymer cantilevers created from dry film resists were to our knowledge first demonstrated by Abgrall *et al* [21] who suspended and patterned self-fabricated, 35  $\mu\text{m}$  thick SU-8 dry resists on a bulk substrate with 3D features. A method fundamentally more similar to ours is the blanket transfer technique demonstrated by Zhang *et al* [22], where self-fabricated dry film photoresists were transferred onto planar substrate surfaces decorated with gaps, leading to partially freestanding photoresist membranes. Polymer cantilevers with thicknesses down to 2  $\mu\text{m}$  were formed in this manner by UV-exposure and development of the photoresist membranes. Their method has the strength of achieving sub-5  $\mu\text{m}$  thick polymer cantilevers, which is advantageous for sensor applications as thinner cantilevers offer increased deflection or force sensitivity as per equation (1). Unfortunately, dry film resists with thicknesses below 5  $\mu\text{m}$  are currently not commercially available, making large scale fabrication of such sub-5  $\mu\text{m}$  polymer cantilevers challenging.

The dry film photoresist used in this work (ADEX<sup>TM</sup>, DJ MicroLaminates), and SU-8 are both epoxy-based, negative tone photosensitive resists. Their chemical resemblances should aid new users of dry resists become familiar with dry film photoresist lithography by taking advantage of decades of SU-8 research. We have for example reported previously that dry film resists also exhibit the *T*-topping effect, caused by strong absorption of UV light in the dry resist top surface during exposure with wavelengths below 350 nm [23]. The two resists' chemical similarities may furthermore enable surface modification of the dry resist by methods previously demonstrated on SU-8. Examples already shown with SU-8 cantilevers include work from the Boisen group on direct adsorption of proteins, as well as single-stranded DNA to the cantilevers without an additional adhesion layer [12, 24]. Strategies to render SU-8 hydrophilic by a facile chemical treatment [25], or extremely hydrophilic by oxygen plasma etching [26] might also be transferrable to dry resists. The Young's moduli of SU-8 and the dry resists used in this work are also similar, and typically 2 to 4 GPa depending on processing conditions related to solvent removal and polymer cross-linking [11, 27, 28].

Demonstrated in this work is the fabrication of plain, one-layer, polymer cantilevers from dry film photoresist with a length ranging from 150  $\mu\text{m}$  to 1000  $\mu\text{m}$ , and aspect ratios up to 1:20. Resulting out-of-plane cantilever deflection as a function of PEB and hardbake was studied, as well as the long-term stability of the developed cantilevers during storage in ambient conditions. To elucidate applications of dry film photoresist cantilevers further, we also fabricated multilayers of dry resist structures. Shown are specifically cylindrical dry resist pillars created on the polymer cantilevers, however any type of multi-layer structure is in principle possible. We show here furthermore, how the integration of a patterned, piezoresistive metal layer on the polymer cantilever is facilitated in our protocols by spin-coating a positive tone photoresist on already exposed, but not yet developed dry resist. The metal is deposited by thermal evaporation, and lift-off yields subsequently the desired metal structures. A proof-of-principle of piezoresistive functionality is demonstrated

by static deflection measurements employing a Wheatstone bridge for accurate voltage read-out. An etching strategy to pattern metal layers on the cantilever is also demonstrated, although care must be taken with regards to material compatibilities during metal etching.

## 2. Materials and methods

### 2.1. Fabrication of AFM compatible silicon probe bodies

Prior to dry resist lamination, substrates containing AFM compatible silicon probe bodies of 3.5 mm  $\times$  1.5 mm length and width, respectively were manufactured in-house relying on a previously demonstrated protocol [23]. First (100)-single-crystalline silicon wafers with 380  $\mu\text{m}$  thickness, double-side covered with 1  $\mu\text{m}$  films of low-stress silicon nitride (figure 1(a)) were cut into 30 mm  $\times$  15 mm pieces, each able to hold 14 AFM-compatible microcantilever probes. UV-photolithography using conventional resist spin-coating and a mask aligner technique was employed to pattern the substrate backside, followed by reactive ion etching (RIE) to remove locally the silicon nitride film (figure 1(b)). The remaining silicon nitride acted as an etch mask during anisotropic KOH etching of the available silicon at 80  $^{\circ}\text{C}$ , forming after 8 h the shape of the probe bodies as well as resulting in 1  $\mu\text{m}$  thick silicon nitride membranes on the substrate front side (figure 1(c)). By complete removal of the front side silicon nitride film in  $\text{CF}_4$ -plasma RIE (figure 1(d)), the silicon probe bodies remained (figure 1(e)). They are attached to a substrate-based frame by two pre-determined breaking points, or bridges, which efficiently fracture when cantilever probes were released by gentle mechanical pressure.

### 2.2. Fabrication of polymer cantilevers by dry film photoresist lithography

Dry film photoresists (ADEX<sup>TM</sup>, DJ MicroLaminates) of 5  $\mu\text{m}$  thickness were exemplary used to create polymer cantilevers utilizing a dry film photoresist lithography protocol. The previously introduced silicon substrates with the AFM probe bodies were cleaned in acetone and isopropanol and dehydrated at 140  $^{\circ}\text{C}$  for 15 min to aid dry resist adhesion. Meanwhile, the dry resist was cut to appropriate sizes with a scissor and the backside protective liner was carefully removed. Substrates were cooled briefly before adhering the dry resist to one of the substrate corners by gentle mechanical pressure. A 1.0 mm thick aluminum carrier plate was used to guide the substrates into a thermal roller laminator at 65  $^{\circ}\text{C}$  with a velocity of 400 mm  $\text{min}^{-1}$  (SKY-DSB 335R6 laminator), homogeneously covering the entire substrate by the dry film photoresist as shown in figure 2(a). Thermal roller lamination proved to be a reliable strategy for dry resist adhesion without diminishing effects such as air bubble formation or substrate fractures. Following thermal lamination, the substrates were placed on a hotplate at 55  $^{\circ}\text{C}$  for 5 min. A glass slide was attached to the substrates' backside by the adhesive Crystalbond 555. Without this back cover, the vacuum clamping of both mask aligner and spin-coater would potentially destroy the suspended dry resist

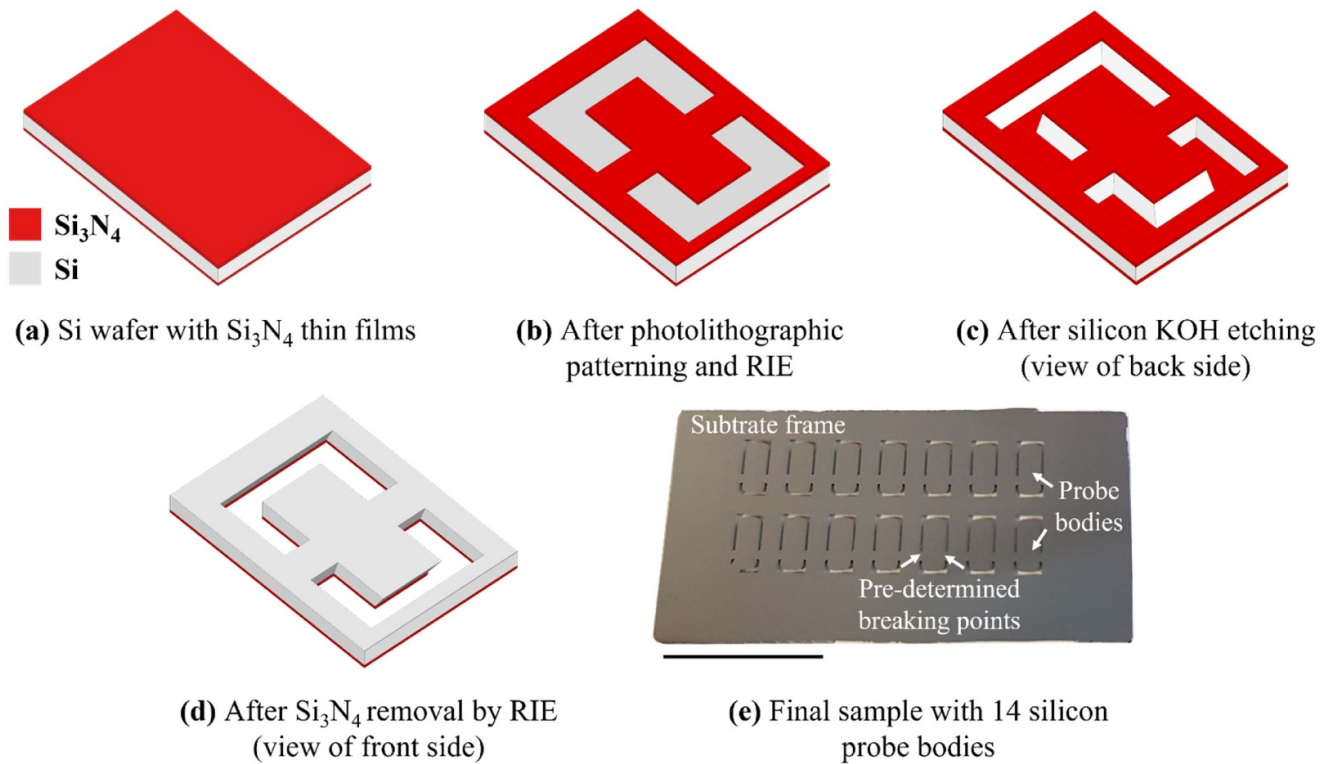


**Figure 1.** Fabrication of AFM compatible silicon probe bodies which act as lamination substrate for the dry film photoresists. (a) A silicon wafer with a double-sided coating of low-stress, LPCVD silicon nitride was used as starting material. (b) Following photolithographic patterning of the backside, silicon nitride was locally removed by CF<sub>4</sub>-RIE to form a suitable etch mask for the (c) subsequent silicon KOH-etch. (d) Removal of the top side silicon nitride completes the fabrication. (e) The final sample displays 14 silicon probe bodies, which are released by gentle mechanical pressure by tweezers after the polymer cantilevers have been fabricated. The length, width and thickness of each probe body is 3.5 mm, 1.5 mm and 380  $\mu\text{m}$  respectively. Scale bar 1 cm.

membranes. A fresh glass slide was consequently attached by Crystalbond prior to each exposure, and eventual spin-coating step required for metal lift-off as described later.

Substrates were exposed for 50 s with the desired cantilever design using a Süß MJB3 mask aligner equipped with an *i*-line filter (power density 3.1  $\text{mW cm}^{-2}$ ). A high exposure dose was chosen to guarantee a complete photoinitiator activation [5, 29], yielding an enhancement of cross-linking homogeneity throughout the cross-sectional area of the dry resist. PEB was performed on a hotplate for 3 h at 60 °C, 15 min at 90 °C and 10 min at 95 °C to evaluate temperature effects. After cooldown, dry resist development was completed in cyclohexanone before rinsing in isopropanol, which yielded directly the free-standing polymer microcantilevers (figure 2(b)). Following probe release by controlled fracture at the pre-determined breaking points on the bulk substrate, the cantilevers' deflection was analyzed by an optical microscope using a specialized sample holder allowing side view imaging.

Released cantilevers were optionally hardbaked in an oven at either 90 °C, 120 °C or 150 °C, at a temperature ramp of approximately 3  $\text{K min}^{-1}$ . Some cantilevers were additionally exposed by UV light (*i*-line, 190  $\text{mJ cm}^{-2}$ ) prior to hardbake for more complete photoinitiator activation, supporting resist cross-linking [5, 29]. Heating was turned off after 15 h and the temperature let to naturally reach below 40 °C. The resulting

cantilever deflection was evaluated shortly after hardbake, and a stability study was conducted for nearly 6 months during which the cantilevers were stored in ambient, dark conditions and measured at regular intervals.

### 2.3. Dry film resist cantilevers with piezoresistive elements made by lift-off technique

Frequently, electroplating [30] or etching [31–33] are used to define (the piezoresistive) metal contacts on spin-coated polymer cantilevers from a previously deposited planar metal film. Instead, we use here the common lift-off technique, which provides increased versatility in terms of material compatibility and eliminates the possibility of severe under-etching during etching protocols.

Dry resist cantilevers, 300  $\mu\text{m}$  in length and 100  $\mu\text{m}$  in width were equipped with a simple piezoresistive element of titanium, to serve purely as a proof-of-concept for both, metalization capabilities and overall piezoresistive functionality. Hence, the piezoresistors span here across the entire microcantilever length rather than being limited to the maximum strain region. Five microns thick dry resists were thermally laminated, exposed with the cantilever design, and post-exposure baked in the previous manner (section 2.2.), only omitting the development in cyclohexanone. A thin film of top antireflection coating, or so-called TARC (AZ Aquaristi III 45) was



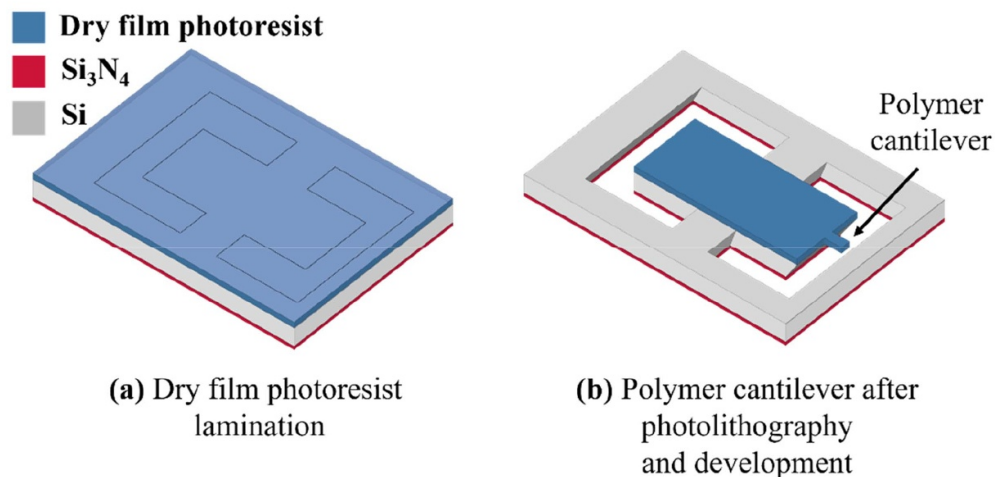


**Figure 2.** (a) Schematic of microfabricated AFM compatible silicon probe bodies embedded in a silicon substrate that is entirely covered by a dry film photoresist. The dry film photoresist is attached to the substrate by thermal roller lamination. (b) Mask aligner UV exposure with the cantilever design, followed by PEB and resist development yields immediately free-standing dry film photoresist cantilevers on the AFM probes without any additional need for a sacrificial layer or other bulk substrate cantilever release strategies.

spin-coated on the exposed dry resist at 4000 rpm for 1 min and baked at 90 °C for 1.5 min. After cool-down, a positive, high-resolution photoresist for lift-off (AZ 701 MIR 29 cp) was spin-coated at 2000 rpm for 1 min, with a 1.75 min soft-bake at 90 °C. The sample was exposed with the metal contacts pattern for 180 s, followed by PEB at 110 °C for 1 min, and development in AZ 726 MIF, which importantly did not attack the dry resist. For improved metal adhesion, the sample was placed in a CF<sub>4</sub>-plasma for 20 s at 95 W power, 3.6·10<sup>-1</sup> mbar pressure and 50 sccm gas flow ( $\mu$ -etch, Plasmalab). A thermal electron-beam evaporator (Temescal FC-1800) was used to deposit 40 nm Ti, which was lifted-off in photoresist remover AZ 100, simultaneously developing the unexposed parts of the dry resist, conveniently resulting in complete piezoresistive polymer probes.

Deflection sensitivity and the resulting Gauge factor were obtained by controlled cantilever probe deflection. Piezoresistive cantilevers were bonded to a Wheatstone bridge on a PCB board, equipped with two identical resistors, denoted *R1* and *R2*, and one variable resistor, *R3*. A needle attached to a micro-manipulator was used to deflect the piezoresistive cantilever downwards in 10  $\mu$ m steps. A source voltage, *V<sub>s</sub>*, of 3 mV was applied over the bridge and the resulting output voltage, *V<sub>m</sub>*, was measured to obtain the deflection sensitivity and Gauge factor of the probe.

#### 2.4. Dry film resist cantilevers with metal structures made by etching techniques

As mentioned previously, metals can also be patterned by an etching strategy, however care must be taken to ensure compatibility of the metal etchant with resists and substrate. As a proof-of-concept, metal lines of nickel were fabricated on the dry resist cantilevers by etching. Following dry resist lamination, UV-exposure and PEB in the previous manner, a 40 nm Ni film was thermally evaporated (Leybold L

560) at 1.33·10<sup>-5</sup> mbar pressure, and maximum 1.5 nm s<sup>-1</sup> deposition rate. An etch mask of positive photoresist (AZ 1512) was spin-coated at 4000 rpm, baked at 90 °C for 3 min, exposed by mask aligner, and developed (AZ 726 MIF). Nickel was etched in a 7:1 solution of HCl:HNO<sub>3</sub> until the desired metal structures formed. The substrate was subsequently developed in cyclohexanone to form cantilevers. Alternatively, the metal was encapsulated after removal of the photoresist etch mask (in AZ 726 MIF), by a thermal lamination of a second layer of 5  $\mu$ m dry resist on top of the patterned substrate. Such metal encapsulation by a so-called passivating layer is important for instance for applications that use the cantilever in liquid environments. UV-exposure, PEB and subsequent development of the two resist layers formed polymer cantilevers with encapsulated metal layers. Reliable encapsulation by the second dry resist requires however high adjustment accuracy of the second photomask layer, and absolute elimination of air-bubbles during the second thermal lamination seems challenging. Both effects are illustrated in figure 3(b).

#### 2.5. Dry film resist cantilevers with integrated polymer microstructures

Multilayer polymer structures are demonstrated with a 150  $\mu$ m × 50  $\mu$ m polymer cantilever forming the first layer, followed by thermal lamination of a second dry resist exposed to form cylindrical pillars. The first 5  $\mu$ m thick dry resist was laminated on the silicon substrate with probe bodies, as outlined in section 2.2. Following UV-exposure and PEB at 95 °C for 10 min to form the shape of the cantilever, a second, 5  $\mu$ m thick dry resist was similarly laminated, exposed with the pillar design, and post-exposure baked in the same fashion. Both resist layers were developed simultaneously in cyclohexanone, and rinsed in isopropanol. A hardbake was performed at 150 °C for 15 h resulting in straight cantilevers.

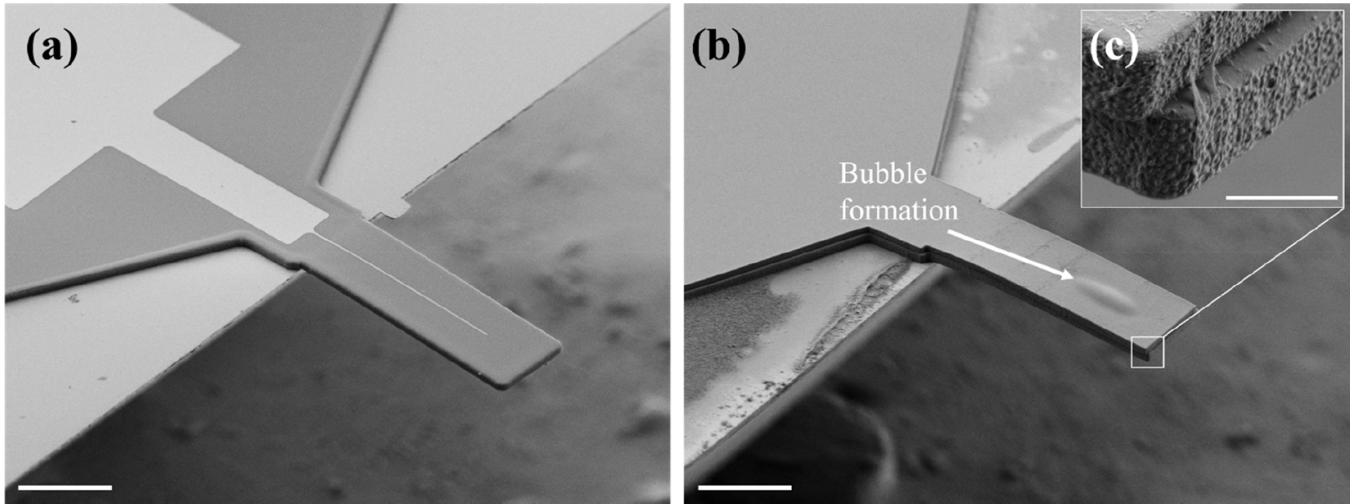


**Figure 3.** (a) A 1.2  $\mu\text{m}$  wide metal line of nickel on a dry resist cantilever produced by an etching strategy. (b) Metal line encapsulated by a second layer of dry resist (albeit not the same cantilever as in (a)). An air bubble formed, and slight alignment errors during exposure of the second photoresist layer are clearly visible in the inset (c). Scale bars (a), (b) 50  $\mu\text{m}$ . Scale bar (c) 5  $\mu\text{m}$ .

### 3. Results and discussion

#### 3.1. Young's modulus and density of dry film resist cantilevers

The spring constants of rectangular dry resist cantilevers were measured with a cantilever calibration device, which requires no previous knowledge of the cantilever geometry or density [34]. Specifically, four dry resist cantilevers of approximately 300  $\mu\text{m}$  length,  $L$  and 100  $\mu\text{m}$  width,  $w$  were measured in air. The width and length of each individual cantilever were measured by an optical microscope, with the geometries of all cantilevers listed in supplementary data table S1 (available online at ([stacks.iop.org/JMM/30/095012/mmedia](http://stacks.iop.org/JMM/30/095012/mmedia))). The cantilever beam thickness was assumed to be 5.0  $\mu\text{m}$  in all cases based on the manufacturer specifications. Note that deviations from the assumed thickness would have an impact to the error evaluations shown later in table 1 of cantilever Young's modulus and density.

The cantilevers were processed at 95  $^{\circ}\text{C}$  PEB, and either: not hardbaked, or hardbaked previously at 130  $^{\circ}\text{C}$ , 140  $^{\circ}\text{C}$  or 150  $^{\circ}\text{C}$  for 15 h, and exhibited bending angles of less than 2 $^{\circ}$  after the finished fabrication. During spring constant measurements, the free-standing end of the polymer cantilever was positioned above a flat-ended,  $\text{\O} 10 \mu\text{m}$  diamond tip and moved down in steps of 0.1  $\mu\text{m}$ . The measurement principle is shown schematically in figure 4, and additional information concerning the measurement setup are provided in the supplementary data.

The applied force to the diamond tip,  $F$  was measured at each deflection during a 10 s integration interval. The spring constant of the cantilever  $k$  represents the slope of the force-distance curve which is calculated by equation (2), where  $\Delta z$  is the applied vertical deflection:

$$k = \frac{\Delta F}{\Delta z}. \quad (2)$$

The loading part of the force–distance curve did not show any non-linear behavior and was used for the spring constant

evaluations. Furthermore, a small hysteresis was observed between loading and unloading of the cantilevers, which might be related to lateral friction forces between tip and cantilever. The spring constants of all four cantilevers were in a similar range, between 499  $\text{mN m}^{-1}$  to 532  $\text{mN m}^{-1}$  (see supplementary data table S1). Note however that the spring constants should not be directly compared to each other due to non-negligible differences in cantilever geometries (table S1). From the spring constants and the cantilevers' geometry, the elastic modulus was obtained by equation (3) which is valid for rectangular beams clamped at one end:

$$E = \frac{4k}{w} \left( \frac{L}{t} \right)^3 \quad (3)$$

where  $t$  is the cantilever thickness, here 5.0  $\mu\text{m}$ . The average elastic modulus of the dry resist cantilevers was  $4.2 \pm 0.2 \text{ GPa}$ , decreasing slightly with increasing hardbake temperature as seen in table 1. A Young's modulus of 3.9 GPa was stated by the producer (DJ MicroLaminates), however can vary depending on processing conditions as stated previously. A larger sample size would however be required for proper evaluation of the effect of hardbake on elastic modulus.

The first three resonance frequencies of dry resist cantilevers were measured by AFM in air which finally allows to determine the density,  $\rho$  of the dry resist cantilevers by equation (4) [35]:

$$f_n = \frac{t \cdot \alpha_n^2}{4\pi L^2} \sqrt{\frac{E}{3\rho}} \quad (4)$$

where  $f_n$  is the  $n^{\text{th}}$  mode resonance frequency. The factor  $\alpha_n$  depends on the mode with the first three factors:

$$\alpha_1 = 1.875 \quad \alpha_2 = 4.694 \quad \alpha_3 = 7.855$$

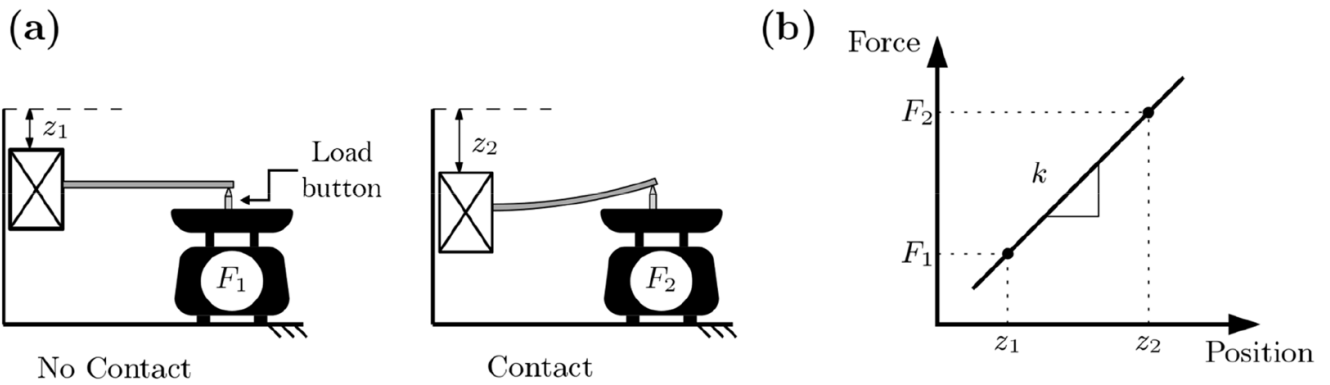


**Figure 4.** (a) Schematic of the cantilever calibration device used for spring constant measurements of the dry film resist cantilevers. The investigated cantilever is positioned above an electromagnetic force compensating (EMFC) balance equipped with a flat-ended diamond tip as load button, which measures the applied force by the cantilever,  $F$ . The cantilever is moved downwards in small increments, from position  $z_1$  to  $z_2$ , while the force is recorded. (b) The slope of the force–distance curve allows the cantilever spring constant,  $k$  to be determined.

**Table 1.** Young’s modulus,  $E$ , and density,  $\rho$ , of dry resist cantilevers processed either without, or with a 15 h hardbake. Spring constants were measured within a cantilever calibration device, while the Young’s modulus and dry resist density were evaluated from the corresponding spring constants by using equation (3) and (5).

Hardbake (°C)	$E$ (GPa)	$\rho$ (g cm <sup>-3</sup> )
-	$4.34 \pm 0.12$	$1.29 \pm 0.03$
130	$4.38 \pm 0.07$	$1.19 \pm 0.02$
140	$4.21 \pm 0.07$	$1.23 \pm 0.02$
150	$3.96 \pm 0.06$	$1.02 \pm 0.02$

Substituting the expression for Young’s modulus from equation (3) into equation (4) yields the simpler expression (5):

$$f_n = \frac{\alpha_n^2}{2\pi} \sqrt{\frac{k}{3wtL\rho}} \quad (5)$$

By fitting the slope of  $f_n(\alpha_n^2)$  for individual cantilevers and their respective spring constants, a dry resist density of  $1.2 \pm 0.1$  g cm<sup>-3</sup> was obtained. There is a significant difference in resist density for the cantilever hardbaked at 150 °C compared to the others, as summarized in table 1. However, a larger sample size is again required to further improve the understanding of hardbake effects on dry resist density. The producer states a dry resist density of 1.03 g cm<sup>-3</sup>, which is close to the range obtained here. Finally, it should be recognized that even small changes in dry resist thickness, dependent for example on hardbake temperature, would significantly influence the error evaluations of both Young’s modulus and dry resist density, but this was not yet investigated.

### 3.2. Effect of PEB and hardbake on dry resist cantilever deflection

Varying PEB temperature and duration, as well as the hardbake temperature had a pronounced effect on the vertical deflection,  $\Delta z$  of the dry resist cantilevers. Following dry resist development in cyclohexanone, but prior to hardbake, all cantilevers

regardless of PEB temperature exhibited negative deflection. That is, the cantilevers were bending towards the probe body as shown in side view in figure 5. Cantilever deflection decreased approximately three-fold for dry resist cantilevers with a 90 °C PEB compared to 60 °C. For the 150  $\mu$ m long, and 50  $\mu$ m wide cantilevers the vertical deflection before hardbake measured  $-12.6 \pm 1.1$   $\mu$ m for 60 °C PEB, and  $-4.1 \pm 0.4$   $\mu$ m for 90 °C PEB (average for 14 cantilevers). After 15 h hardbake at 90 °C, 120 °C or 150 °C, low-temperature cantilevers, with a 60 °C PEB showed a pronounced increase in absolute vertical deflection, while at higher PEB temperatures of 90 °C, cantilevers showed a decrease in absolute deflection. Only two cantilevers of each PEB temperature type were processed at the same hardbake conditions, and results from these individual probes in terms of deflection change following hardbake at different temperatures are shown in figure 6.

Stress and deflection behavior of SU-8 cantilevers by the spin-coating method was investigated by other research groups [5, 13, 36]. Notably, Keller *et al* [5] argued for 2  $\mu$ m thick SU-8 cantilevers that the bending behavior of the released, thin cantilevers is hardly caused by neither: gradients in received UV-dose across the resist film, temperature gradients in the resist during PEB, or polymer shrinkage during PEB cross-linking, which are all more relevant factors to consider for thicker resist films. Differences in thermal properties between 2  $\mu$ m, and 5  $\mu$ m thick resist films should furthermore be negligible [13]. However, solvent gradients in the resist after PEB, caused by differences in solvent evaporation rates between the outer and inner parts of the resist appeared critical. Generally, at lower temperatures, the solvent concentration in the bulk of the resist increases relative to the outer resist surface. As high solvent concentrations promote resist cross-linking more readily, this causes the resist surface to contract during cool-down leading to a more pronounced cantilever deflection. Enhanced cantilever deflection is consequently an issue at lower  $T_{PEB}$ , with deflection directed away from the substrates in the case of spin-coated SU-8 cantilevers. We observed however the inverse behavior with dry resist cantilevers, with cantilevers bending towards, instead of away from the substrates.



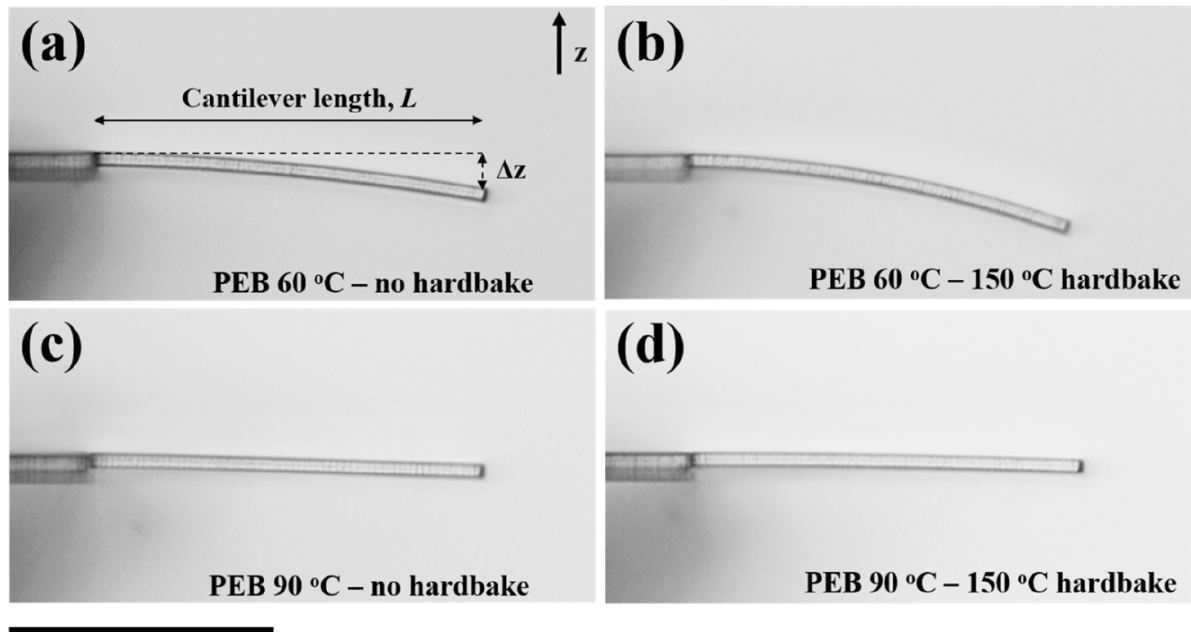


**Figure 5.** (a), (b) Dry resist cantilever processed at 60 °C PEB, before and after a hardbake at 150 °C, respectively. (c), (d) Dry resist cantilever processed at 90 °C PEB, before and after a hardbake at 150 °C, respectively. Generally, increased PEB temperature generates less bending following dry resist development. A subsequent hardbake generates even more negative deflection on dry resist cantilevers with a 60 °C PEB compared to 90 °C, where in the latter case the absolute vertical deflection decreases. Scale bar 100 μm.

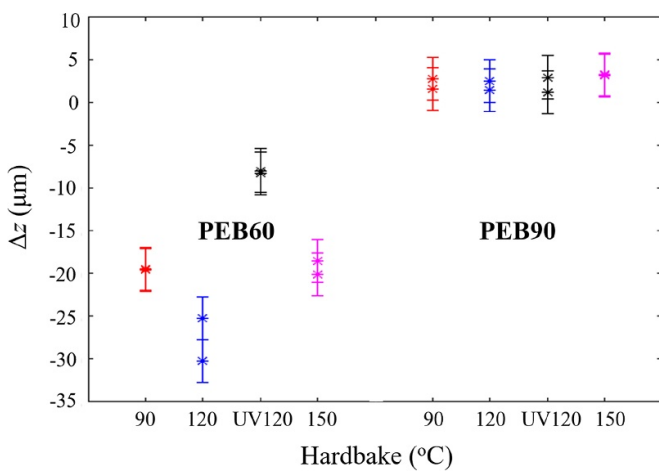


**Figure 6.** Change in vertical deflection,  $\Delta z$  for 150 μm long, 50 μm wide dry resist cantilevers processed at either 60 °C or 90 °C PEB, following a hardbake at either at 90 °C, 120 °C or 150 °C. Negative values indicate downwards deflection, towards the probe body. Two cantilevers from the same substrate, with identical PEB, were hardbaked with the same conditions. Some cantilevers were additionally flood exposed with a high UV dose prior to hardbake to activate photoinitiator compounds in the resist (see UV120). This evidently has the effect of decreasing beam deflection of 60 °C PEB cantilevers compared to cantilevers without the UV-pretreatment.

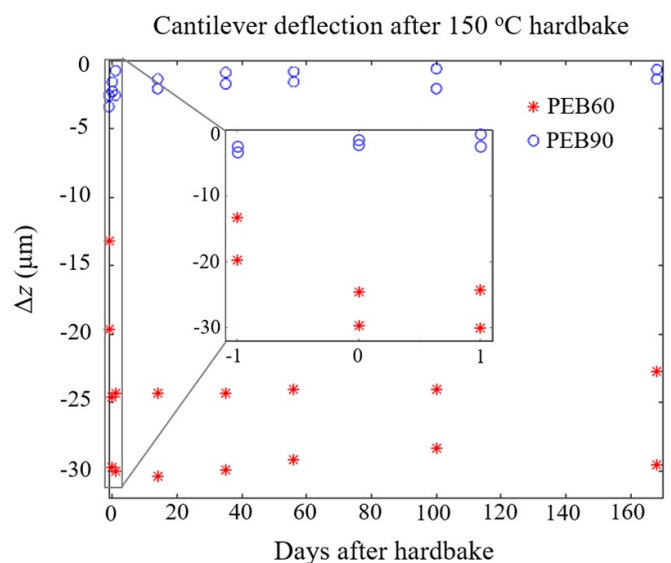


**Figure 7.** Time-stability of 150 μm long and 50 μm wide dry resist cantilevers with PEB at either, 60 °C (PEB60) or 90 °C (PEB90), and hardbaked at 150 °C, up to approximately half a year after hardbake. Day “-1” indicates deflection prior to hardbake. Day “0” is measured directly after cool-down from the hardbake. No significant change in cantilever deflection was observed with time. The measurement points are accurate to  $\pm 2.5$  μm.

The difference in bending behavior is most likely due to the different geometrical scenarios. While spin-coated cantilevers are in full contact with the planar substrate, dry resist cantilevers are formed here from suspended dry resist membranes. Intuitively, solvent is able to escape from both surfaces of the dry resist membranes, ideally causing

an isotropic solvent gradient in the resist and thus straight cantilevers. The temperature differences between the top and bottom of the suspended dry resist are neglected. However, solvent gradients are expected at the interface between dry resist on the silicon probe body and the adjacent suspended dry resist. A resulting cross-linking gradient at the base of the

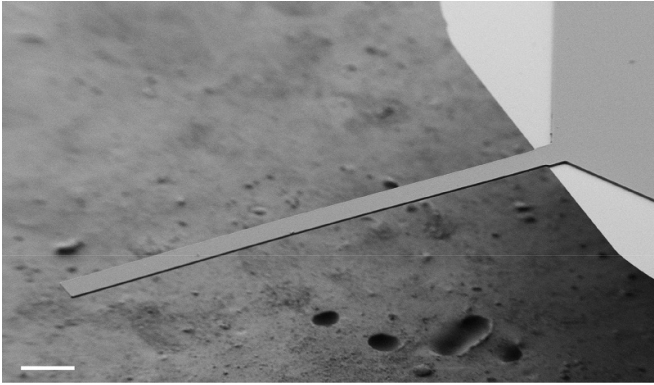


**Figure 8.** 1000  $\mu\text{m}$  long, 50  $\mu\text{m}$  wide polymer cantilever with excellent in-plane-alignment following a hardbake at 150  $^{\circ}\text{C}$ . Scale bar 100  $\mu\text{m}$ .

cantilevers could explain partly why developed dry resist cantilevers can be under stress.

Also important for the observed bending behavior of dry resist cantilevers are likely the complex interactions of thermal properties between the silicon substrate and dry resist. Silicon heat conduction is approximately four orders of magnitude larger than for air, meaning dry resist directly attached to the silicon substrate heats up considerably faster than the suspended dry resist membranes. Furthermore, the coefficient of thermal expansion of dry resists is two orders of magnitude smaller than for silicon, indicating that the thin dry resists undergo tensile stress during heating. However, while assuming the occurrence of flow during substrate heating, the dry film resist might end up in a compressed state at the end of the cooling cycle back to room temperature. The combination in differences of heat conduction, and thermal expansion are complicated to understand and to relate to dry resist membrane behavior during PEB without simulation studies. Fourier-transform infrared spectroscopy (FT-IR) could furthermore be used in future to evaluate resist cross-linking densities, as it was already demonstrated with the similar SU-8 resist [37]. In either case the situation is not as straightforward as for polymer cantilevers spin-coated on planar substrates. Computational simulations could in future help to improve the understanding of the dry resist membranes' behavior during PEB and thereby provide valuable information to further improve the fabrication process, e.g. in terms of PEB temperature and ramp, and if PEB in an oven would provide a better option to reduce cross-linking gradients in the dry resist membranes.

Additionally, the lamination process could be considered affecting cantilever deflection. The manner at which the dry resist adheres to the substrate is not precisely controlled, and differences might arise in the local bonding quality of the dry resist membranes that are stretched across the silicon substrate 3D-surfaces. To exclude variability of roller lamination, a test was performed where dry resists were laminated either with the thermal roller laminator, or allowed to self-laminate onto the substrate. Here instead of thermal roller lamination the dry resist was just mechanically attached to a corner of

the substrate, placed on at hotplate at 65  $^{\circ}\text{C}$ , and allowed to self-adhere without applying any external force on the dry resist film. The two samples, roller laminated and self-laminated, were processed in the same manner by UV-exposure, PEB and development. No differences in cantilever deflection between the two samples were observed neither after development, nor after hardbake at different temperatures, indicating that the choice of lamination technique is more or less irrelevant for the resulting cantilever deflection. But it should be noted that other researchers have found precise control of lamination temperature and pressure to be decisive for obtaining optimal resist structures [21].

Hardbaking has the same effect on both spin-coated cantilevers [5], and high temperature, 90  $^{\circ}\text{C}$  PEB dry resist cantilevers, with the hardbake reducing out-of-plane deflection (see figures 5 and 6). This effect has been related to solvent removal from the bulk of the resist, and more homogenous cross-linking density of the whole polymer cantilever [5, 36]. Figure 6 furthermore reveals that particularly cantilevers with a low temperature, 60  $^{\circ}\text{C}$  PEB experience a significant absolute reduction in resulting out-of-plane deflection following hardbake (at 120  $^{\circ}\text{C}$ ) when initially treated with a high UV dose, compared to similar 60  $^{\circ}\text{C}$  PEB cantilevers not additionally exposed by UV light. This indicates that 60  $^{\circ}\text{C}$  PEB cantilevers have a significant degree of non-crosslinked resist prior to hardbake, as the UV treatment and subsequent increase in photoinitiator helps make cross-linking density more homogenous resulting in less bending.

Curiously, all cantilevers with a low temperature PEB (60  $^{\circ}\text{C}$ ) increase their bending after the hardbake, regardless of hardbake temperature and UV treatment. Additionally, these cantilevers experience approximately the same deflection increase following a hardbake at either 90  $^{\circ}\text{C}$  and 150  $^{\circ}\text{C}$ , while at the middle temperature of 120  $^{\circ}\text{C}$  the cantilevers deflect the most relative to the original value. In order to verify that the 3 h PEB duration at 60  $^{\circ}\text{C}$  was neither too long, potentially causing damage to the resist chemistry, or too short and incapable of achieving high cross-linking density, additional samples were fabricated in the same manner while employing PEB durations of either 1 h, 2 h, 7 h, or 15 h. No adverse effects were experienced by shorter or longer PEB durations. Cantilevers were properly developed even after 1 h PEB, and no tears in the dry resist membranes were observed after 15 h. Nevertheless, the bending behavior of cantilevers following hardbake did not change relative to the standard 3 h long PEB process. That is, improper PEB duration is not the cause of increased negative deflection following hardbake. Rather it seems likely that PEB at 60  $^{\circ}\text{C}$  provides too little energy for proper cross-linking of exposed dry resist, leading by an unknown mechanism to a deflection increase after hardbake. This mechanism might, as discussed previously, be related to the complex sample structure.

To evaluate the long term stability, a nearly six month stability study of the released dry resist cantilevers was done and showed the original deflection to be maintained, both for cantilevers with and without hardbake. Results for either PEB at a hardbake of 150  $^{\circ}\text{C}$  is shown in figure 7. This corresponds to results from Martin *et al* [17] who irrespective of

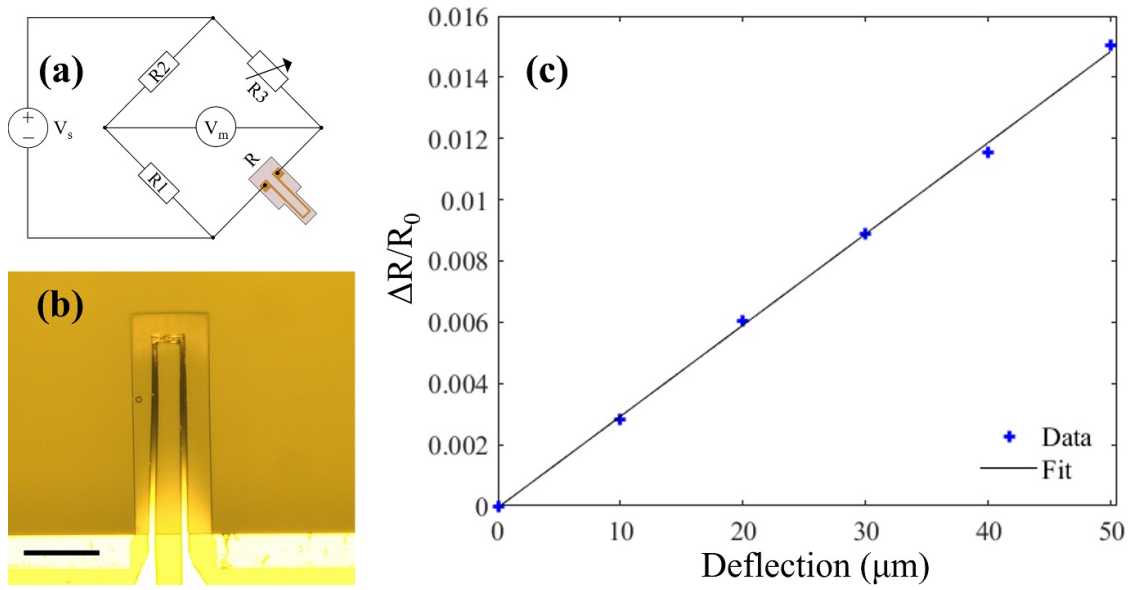


**Figure 9.** (a) Wheatstone bridge setup, with three resistors R1, R2 and R3 and the piezoresistive cantilever, R. A potential,  $V$  is applied and the bridge potential,  $V_m$  is measured. (b) Typical top side view of 300  $\mu\text{m}$  long dry resist cantilever with piezoresistive Ti metal contacts. Scale bar 100  $\mu\text{m}$ . (c) Deflection sensitivity of the piezoresistive dry resist cantilever achieving  $298 \text{ m}^{-1}$  with indicated linear fit.

PEB temperature also did not observe changes in SU-8 cantilever deflection following one year after release.

Based on the results we fabricated 1000  $\mu\text{m}$  long, 50  $\mu\text{m}$  wide cantilevers from 5  $\mu\text{m}$  thick dry resists as seen in figure 8. Using a PEB of 95  $^\circ\text{C}$  to reduce initial cantilever deflection, and UV flood exposure prior to a hardbake at 150  $^\circ\text{C}$  for 15 h, resulting dry resist cantilevers exhibited a minimal vertical deflection at their free-standing ends of only 1  $\mu\text{m}$ . Long polymer cantilevers are favourable to realize highly sensitive chemical sensors based on the differential surface stress principle, as by equation (1).

### 3.3. Piezoresistive dry resist cantilevers

Equivalent resistance values of the piezoresistive cantilever,  $R$  were calculated from the source voltage,  $V_s$  and measured output voltage,  $V_m$  by the below equation (6) [38].  $R_3$  is the resistance of the variable resistor.

$$R = R_3 \times \frac{2V_m + V_s}{V_s - 2V_m} \quad (6)$$

The deflection sensitivity was obtained from the slope of  $\Delta R/R_0$  as a function of vertical displacement (figure 9), where  $R_0$  is the resistance prior to deflection. A value of  $298 \text{ m}^{-1}$  was obtained, similar to what was reported previously in literature [3, 32], albeit with both different geometries and piezoresistive materials. The Gauge factor,  $K$  of the cantilever was calculated from the deflection sensitivity and geometric considerations as by the following equation:

$$\frac{\left(\frac{\Delta R}{R_0}\right)}{z} = K \times \frac{3t(l-L/2)}{2l^3} \quad (7)$$

where  $L$  and  $l$  are the cantilever and piezoresistor lengths respectively, and  $t$  is cantilever thickness. For the specific geometry used here a Gauge factor of 6.2 was obtained.

Improved photolithography protocols to enhance metal adhesion to the dry resist film with the lift-off technique are currently under investigation. Notably, the complete removal of exposed positive photoresist, AZ 701 MIR, is not easy within the current scheme, and commonly leaves photoresist residues, which cannot be removed during development (figure 10). This makes achieving high probe yields challenging. An increased exposure time, varying the TARC thickness, using TARC also on-top of the positive resist, decreasing the positive photoresist thickness by half by spin-coating at 6000 rpm instead of 2000 rpm, varying soft-bake temperatures and durations, increasing the rehydration time after softbake as well as the time between exposure and PEB of the positive photoresist were tested with variable success, yielding eventually the current protocol. Filling the air gaps between photomask and sample by near-index matching liquid (glycerol) was also attempted to minimize diffraction effects, but yielded no notable improvements to resist development. Recently, we had some advances in properly developing the positive resist by spin-coating TARC before dry resist PEB. This suggest also some loss of dry resist planarity during PEB, causing an uneven surface and irregular spin-coating conditions of the TARC and positive resist.

Notably, the use of TARC was crucial to ensure improved photoresist exposure, even though we suspect better mask aligner wedge-edge compensation and use of a high-resolution positive resist compatible with broadband UV-exposure might reduce the effects of back-reflected UV-light and the resulting interference effects. Optimizing the cantilever substrate design to avoid using the partly non-planar glass with Crystalbond as



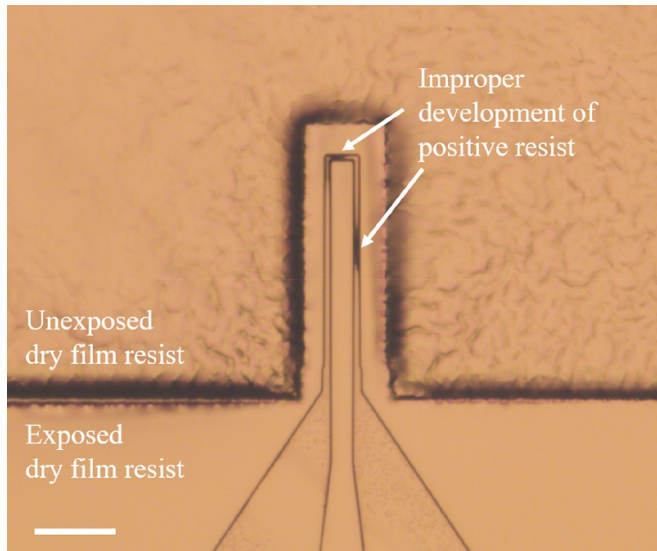


**Figure 10.** Improper removal of exposed positive photoresist following development. The dark marks in the contacts area indicated by the arrows seem to be remnant photoresist. Prolonged resist development did not help removal. Scale bar 100  $\mu\text{m}$ .

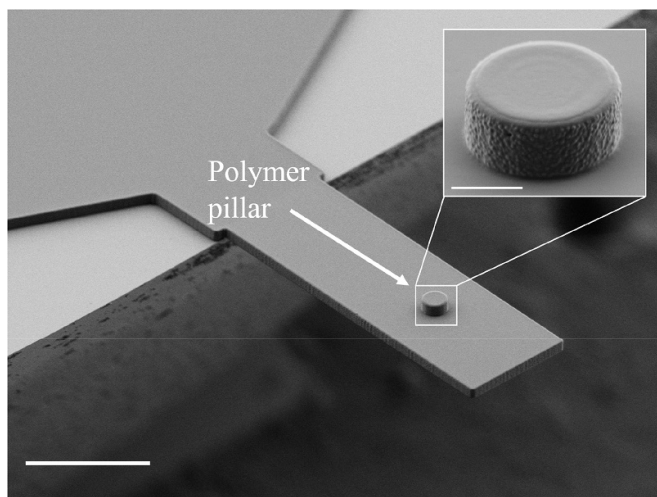


**Figure 11.** Dry resist cantilever with a flat-ended polymer pillar structured from a second layer of dry resist. The pillar exhibits the same morphology as in previous work [23], with bumps at side-walls and an elevated rim on the resist top-surface. Scale bar overview 50  $\mu\text{m}$ . Scale bar inset 5  $\mu\text{m}$ .

a protective backside would also be integral to reduce interference effects.

### 3.4. Multilayer resist structures—dry resist cantilever with cylindrical dry resist tip

A polymer cantilever with a cylindrical polymer pillar is shown in figure 11, and was processed at a 95 °C PEB. Deflection prior to hardbake was  $-5.5 \pm 1.1 \mu\text{m}$ . After a hardbake at 150 °C the cantilevers showed an average bending of  $1.0 \pm 0.7 \mu\text{m}$ . Multilayer polymer structures could be used to realize scanning tips [23], hollow polymer cantilevers for microbeads or cell manipulation and cell measurements

[39–41], and for passivation/encapsulation layers of metallic contacts as demonstrated previously (see figure 3).

## 4. Conclusion

A novel method to create AFM compatible polymer microcantilevers on durable silicon probe bodies was demonstrated, albeit the method is in principle also applicable for other probe body platforms serving original end-user applications. UV photolithography of partly suspended dry film photoresists forms polymer cantilevers directly by resist development, and importantly eliminates bulk substrate release, which frequently causes plastic deformation to polymer probes fabricated by spin-coating. The new method furthermore requires no more than two thermal cycles, the PEB and an optional hardbake.

Cantilever spring constants were directly measured with a high-accuracy cantilever calibration device. By knowing the spring constants, cantilever Young's moduli and density were conveniently calculated, yielding values of 4 GPa to 4.4 GPa and  $1.0 \text{ g cm}^{-3}$  to  $1.3 \text{ g cm}^{-3}$  respectively, depending on previous processing conditions. Evaluations on the effect of bake temperatures demonstrated that both a high temperature PEB, above 90 °C, and high hardbake temperatures, above 120 °C are desirable to limit vertical deflection of the dry film resist cantilevers. Using an optimized protocol we were able to fabricate 5  $\mu\text{m}$  thick, 1000  $\mu\text{m}$  long cantilevers displaying only 1  $\mu\text{m}$  maximal deflection providing theoretically high deflection sensitivities for future chemical and biochemical sensing applications. Polymer cantilevers from dry film photoresist can be furthermore, patterned with metals using conventional lift-off or etching protocols. This could in future support the realization of polymeric dry film resist cantilevers with an integrated piezoresistive readout, and a first proof-of-principle was already demonstrated here realizing a deflection sensitivity of  $298 \text{ m}^{-1}$ .

Multilayer polymer structures with the polymer cantilever comprising the first layer were also realized. Specifically the fabrication of a cylindrical polymer pillar on top of the polymer cantilever was shown, where both photoresist layers were developed simultaneously.

Dry film photoresist technology needs to evolve in order to produce cantilevers thinner than 5  $\mu\text{m}$ , which is the thinnest dry film photoresist on the commercial market today. At 5  $\mu\text{m}$  film thickness the advantageous properties of the low Young's modulus are lost compared to for instance much thinner silicon nitride cantilevers of same length and width. However with the advances in recent years in producing ever thinner dry film photoresists, the future might see sub-5  $\mu\text{m}$  commercially available dry resists, capable of producing even more sensitive polymer probes as well as achieving improved patterning resolution.

## Acknowledgments

The financial support by the Ministry of Education and Research Germany (BMBF: NanoMatFutur: 13N12545) is gratefully acknowledged. Furthermore, we thank S Hettich



and S Jenisch at Ulm University for their experimental support and technical assistance.

## ORCID iDs

Madeleine Nilsen  <https://orcid.org/0000-0003-3035-4718>

Steffen Strehle  <https://orcid.org/0000-0002-1261-2894>

## References

- [1] Gad-el-hak M 2005 *MEMS: Introduction and Fundamentals* (Boca Raton, FL: CRC Press)
- [2] Madou M J 2002 *Fundamentals of Microfabrication: The Science of Miniaturization* 2nd edn (Boca Raton, FL: Taylor & Francis)
- [3] Mathew R and Ravi Sankar A 2018 A review on surface stress-based miniaturized piezoresistive SU-8 polymeric cantilever sensors *Nano-Micro Lett.* **10** 35
- [4] Nemani K V, Moodie K L, Brennick J B, Su A and Gimi B 2013 *In vitro* and *in vivo* evaluation of SU-8 biocompatibility *Mater. Sci. Eng. C* **33** 4453–9
- [5] Keller S, Haefliger D and Boisen A 2010 Fabrication of thin SU-8 cantilevers: initial bending, release and time stability *J. Micromech. Microeng.* **20** 045024
- [6] Patil S J, Duragkar N and Rao V R 2014 An ultra-sensitive piezoresistive polymer nano-composite microcantilever sensor electronic nose platform for explosive vapor detection *Sensors Actuators B* **192** 444–51
- [7] Reddy C V B, Khaderbad M A, Gandhi S, Kandpal M, Patil S, Chetty K N, Rajulu K G, Chary P C K, Ravikanth M and Rao V R 2012 Piezoresistive SU-8 cantilever with Fe(III)porphyrin coating for CO sensing *IEEE Trans. Nanotechnol.* **11** 701–6
- [8] Patil S J, Adhikari A, Baghini M S and Rao V R 2014 An ultra-sensitive piezoresistive polymer nano-composite microcantilever platform for humidity and soil moisture detection *Sensors Actuators B* **203** 165–73
- [9] Nordström M, Zauner D A, Calleja M, Hübner J and Boisen A 2007 Integrated optical readout for miniaturization of cantilever-based sensor system *Appl. Phys. Lett.* **91** 103512
- [10] Genolet G, Brugger J, Despont M, Drechsler U, Vettiger P, de Rooij N F and Anselmetti D 1999 Soft, entirely photoplastic probes for scanning force microscopy *Rev. Sci. Instrum.* **70** 2398–401
- [11] Hopcroft M, Kramer T, Kim G, Takashima K, Higo Y, Moore D and Brugger J 2005 Micromechanical testing of SU-8 cantilevers *Fatigue Fract. Eng. Mater. Struct.* **28** 735–42
- [12] Nordström M, Keller S, Lillemose M, Johansson A, Dohn S, Haefliger D, Blagoi G, Havsteen-Jakobsen M and Boisen A 2008 SU-8 cantilevers for bio/chemical sensing: fabrication, characterisation and development of novel read-out methods *Sensors* **8** 1595–612
- [13] Lim Y C, Kouzani A Z, Kaynak A, Dai X J, Littlefair G and Duan W 2015 A protocol for improving fabrication yield of thin SU-8 microcantilevers for use in an aptasensor *Microsyst. Technol.* **21** 371–80
- [14] Keller S, Haefliger D and Boisen A 2007 Optimized plasma-deposited fluorocarbon coating for dry release and passivation of thin SU-8 cantilevers *J. Vac. Sci. Technol. B* **25** 1903–8
- [15] Jun-Hyung A, Chang-Sin P and Dong-Weon L 2010 Fabrication of a wheatstone-bridge integrated SU-8 cantilever *Jpn. J. Appl. Phys.* **49** 06GN1
- [16] Kim J Y, Choi Y-S, Lee B-K and Lee D-W 2016 Surface-patterned SU-8 cantilever arrays for preliminary screening of cardiac toxicity *Biosens. Bioelectron.* **80** 456–62
- [17] Martin C, Llobera A, Villanueva G, Voigt A, Gruetzner G, Brugger J and Perez-Murano F 2009 Stress and aging minimization in photoplastic AFM probes *Microelectron. Eng.* **86** 1226–9
- [18] Mouaziz S, Boero G, Popovic R S and Brugger J 2006 Polymer-based cantilevers with integrated electrodes *J. Microelectromech. Syst.* **15** 890–5
- [19] Ransley J H T, Watari M, Sukumaran D, McKendry R A and Seshia A A 2006 SU8 bio-chemical sensor microarrays *Microelectron. Eng.* **83** 1621–5
- [20] Nordström M 2004 Fabrication of cantilever chip with complementary micro channel system in SU-8 for biochemical detection *MSc Thesis* Lund University & Technical University of Denmark
- [21] Abgrall P, Charlot S, Fulcrand R, Paul L, Boukabache A and Gué A-M 2008 Low-stress fabrication of 3D polymer free standing structures using lamination of photosensitive films *Microsyst. Technol.* **14** 1205–14
- [22] Zhang Y, Han J-H, Zhu L, Shannon M A and Yeom J 2014 Soft lithographic printing and transfer of photosensitive polymers: facile fabrication of free-standing structures and patterning fragile and unconventional substrates *J. Micromech. Microeng.* **24** 115019
- [23] Nilsen M, Port F, Roos M, Gottschalk K-E and Strehle S 2019 Facile modification of freestanding silicon nitride microcantilever beams by dry film photoresist lithography *J. Micromech. Microeng.* **29** 025014
- [24] Marie R, Schmid S, Johansson A, Ejsing L, Nordström M, Häfliger D, Christensen C B V, Boisen A and Dufva M 2006 Immobilisation of DNA to polymerised SU-8 photoresist *Biosens. Bioelectron.* **21** 1327–32
- [25] Nordström M, Marie R, Calleja M and Boisen A 2004 Rendering SU-8 hydrophilic to facilitate use in micro channel fabrication *J. Micromech. Microeng.* **14** 1614
- [26] Ferdinand W, Polina D, Stefan Z, Michael K, Helmut H, Alexander M G and Robert W S 2007 Stability of the hydrophilic behavior of oxygen plasma activated SU-8 *J. Micromech. Microeng.* **17** 524
- [27] Robin C J and Jonnalagadda K N 2016 Effect of size and moisture on the mechanical behavior of SU-8 thin films *J. Micromech. Microeng.* **26** 025020
- [28] Robin C J, Vishnoi A and Jonnalagadda K N 2014 Mechanical behavior and anisotropy of spin-coated SU-8 thin films for MEMS *J. Microelectromech. Syst.* **23** 168–80
- [29] Mitra S K and Chakraborty S 2011 *Microfluidics and Nanofluidics Handbook: Fabrication, Implementation, and Applications* (Boca Raton, FL: Taylor & Francis)
- [30] Johansson A, Calleja M, Rasmussen P A and Boisen A 2005 SU-8 cantilever sensor system with integrated readout *Sensors Actuators A* **123–124** 111–5
- [31] Thaysen J, Yalçinkaya A D, Vettiger P and Menon A 2002 Polymer-based stress sensor with integrated readout *J. Phys. D: Appl. Phys.* **35** 2698
- [32] Shokuhfar A, Heydari P, Aliahmadi M R, Mohtashamifar M, Ebrahimi-Nejad R S and Zahedinejad M 2012 Low-cost polymeric microcantilever sensor with titanium as piezoresistive material *Microelectron. Eng.* **98** 338–42
- [33] Seena V, Rajorya A, Pant P, Mukherji S and Rao V R 2009 Polymer microcantilever biochemical sensors with integrated polymer composites for electrical detection *Solid State Sci.* **11** 1606–11
- [34] Diethold C, Kühnel M, Hilbrunner F, Fröhlich T and Manske E 2014 Determination of force to displacement curves using a nanopositioning system based on electromagnetic force compensated balances *Measurement* **51** 343–8

- [35] Gorman D G and Kennedy W 1988 *Applied Solid Dynamics* (London: Butterworths)
- [36] Sameoto D, Tsang S H, Foulds I G, Lee S W and Parameswaran M 2007 Control of the out-of-plane curvature in SU-8 compliant microstructures by exposure dose and baking times *J. Micromech. Microeng.* **17** 1093–8
- [37] Keller S, Blagoi G, Lillemose M, Haeffiger D and Boisen A 2008 Processing of thin SU-8 films *J. Micromech. Microeng.* **18** 125020
- [38] National-Instruments 2019 *Measuring Strain With Strain Gages* [www.ni.com/de-de/innovations/white-papers/07/measuring-strain-with-strain-gages.html](http://www.ni.com/de-de/innovations/white-papers/07/measuring-strain-with-strain-gages.html) (Accessed 04 02 2020)
- [39] Han H, Martinez V, Aebersold M J, Luchtefeld I, Polesel-Maris J, Vörös J and Zambelli T 2018 Force controlled SU-8 micropipettes fabricated with a sideways process *J. Micromech. Microeng.* **28** 095015
- [40] Martinez V, Behr P, Drechsler U, Polesel-Maris J, Potthoff E, Vörös J and Zambelli T 2016 SU-8 hollow cantilevers for AFM cell adhesion studies *J. Micromech. Microeng.* **26** 055006
- [41] Martinez V, Forró C, Weydert S, Aebersold M J, Dermutz H, Guillaume-Gentil O, Zambelli T, Vörös J and Demkó L 2016 Controlled single-cell deposition and patterning by highly flexible hollow cantilevers *Lab Chip* **16** 1663–74